

Supporting Information

Ultrathin FeOOH Nanosheets as an Efficient Cocatalyst for Photocatalytic Water Oxidation

Ge Ge,^{ab} Min Liu,^{ab} Chao Liu,^{ab} Wei Zhou,^c Defa Wang,^{ab} Lequan Liu,^{*ab} and Jinhua Ye,^{*abd}

^aTJU-NIMS International Collaboration Laboratory, Key Lab of Advanced Ceramics and Machining Technology (Ministry of Education) and Tianjin Key Laboratory of Composite and Functional Materials, School of Material Science and Engineering, Tianjin University, 92 Weijin Road, Tianjin, P. R. China.

^bCollaborative Innovation Center of Chemical Science and Engineering (Tianjin), Tianjin 300072, People's Republic of China.

E-mail: Lequan.Liu@tju.edu.cn

^cDepartment of Applied Physics, Tianjin Key Laboratory of Low Dimensional Materials Physics and Preparing Technology, Faculty of Science, Tianjin University, Tianjin 300072, P. R. China.

^dInternational Center for Materials Nanoarchitectonics (WPI-MANA), National Institute for Materials Science (NIMS) 1-1 Namiki, Tsukuba, Ibaraki 3050044, Japan.

E-mail: Jinhua.Ye@nims.go.jp

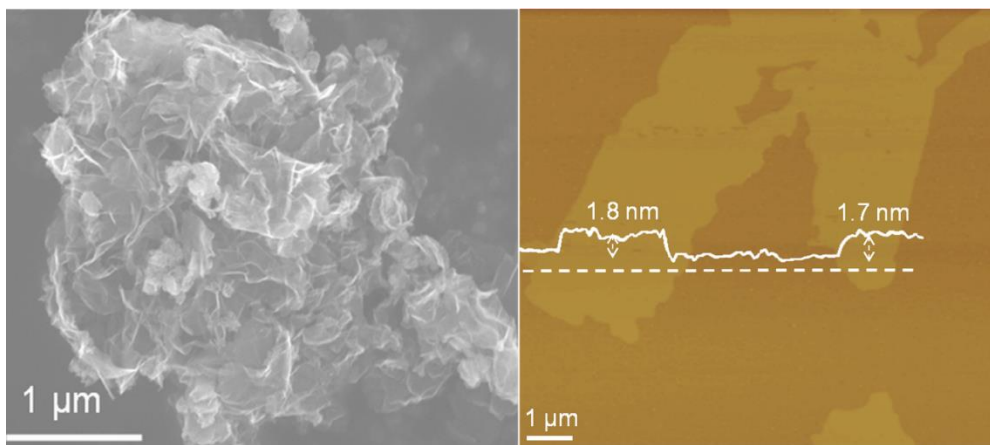


Fig. S1 SEM and AFM images of ultrathin FeOOH NSs.

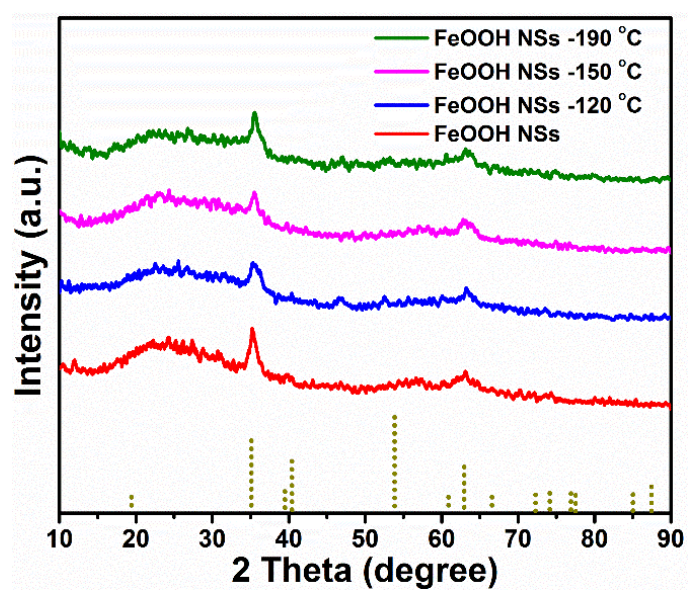


Fig. S2 XRD patterns of ultrathin FeOOH nanosheets with different heat treatment temperature.

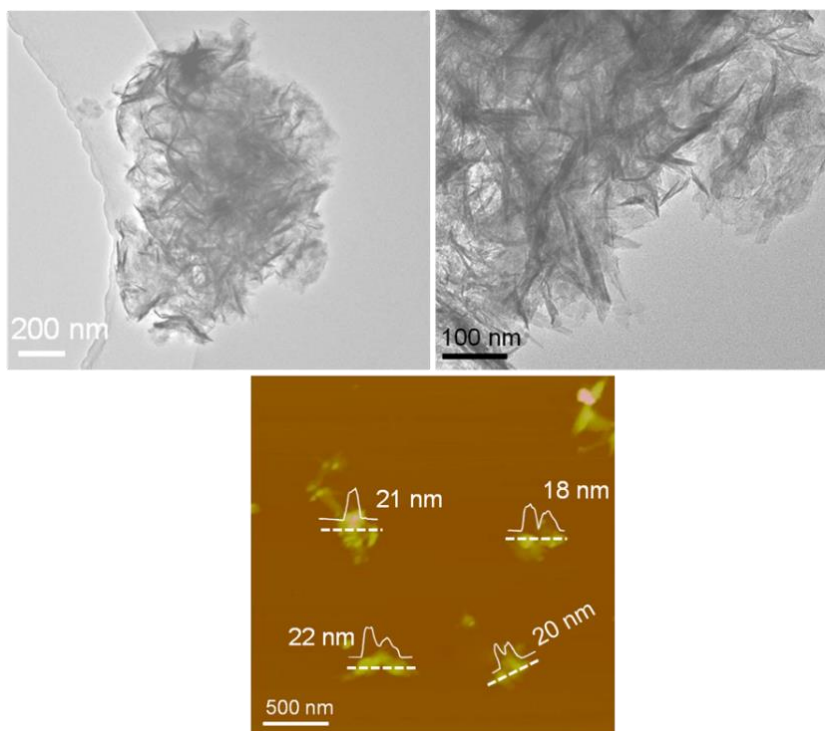


Fig. S3 TEM and AFM images of FeOOH q-NSs.

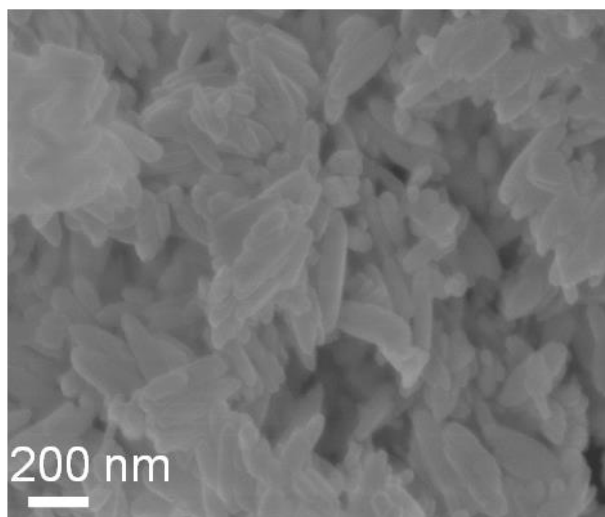


Fig. S4 SEM image of FeOOH bulk.

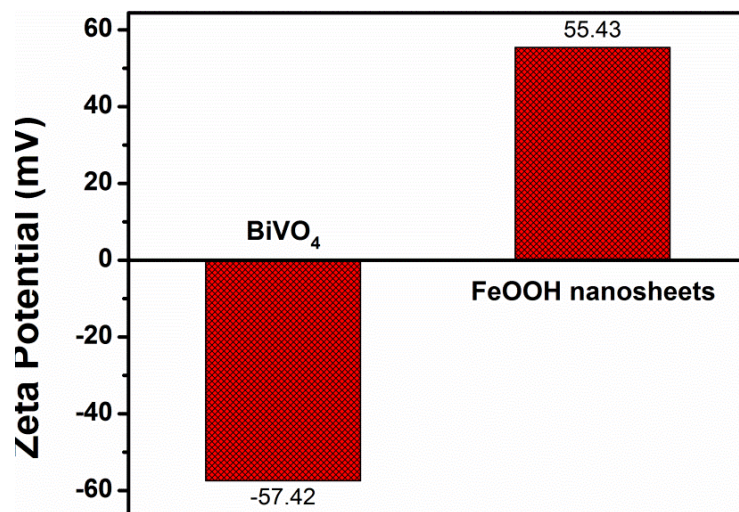


Fig. S5 Zeta potentials of BiVO₄ and ultrathin FeOOH NSs.

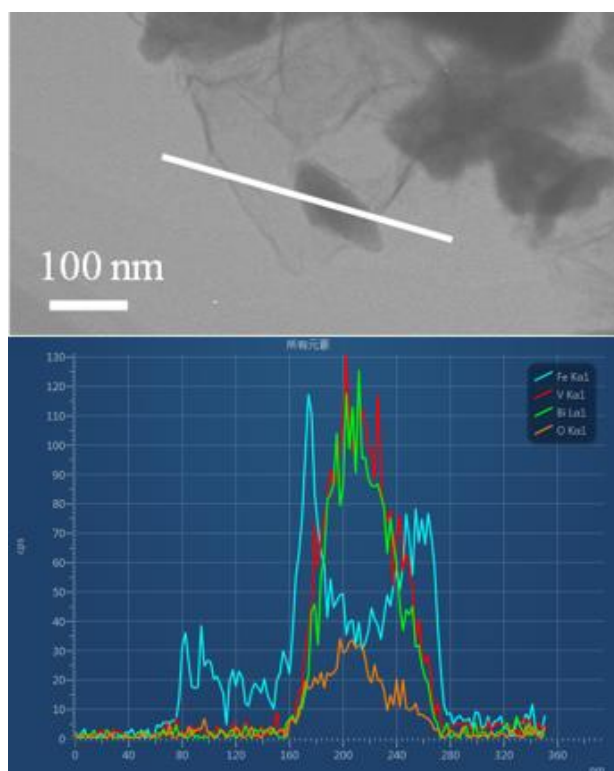


Fig. S6 EDX line scanning analysis with white line in TEM image showing the element distribution of Bi, V, O and Fe.

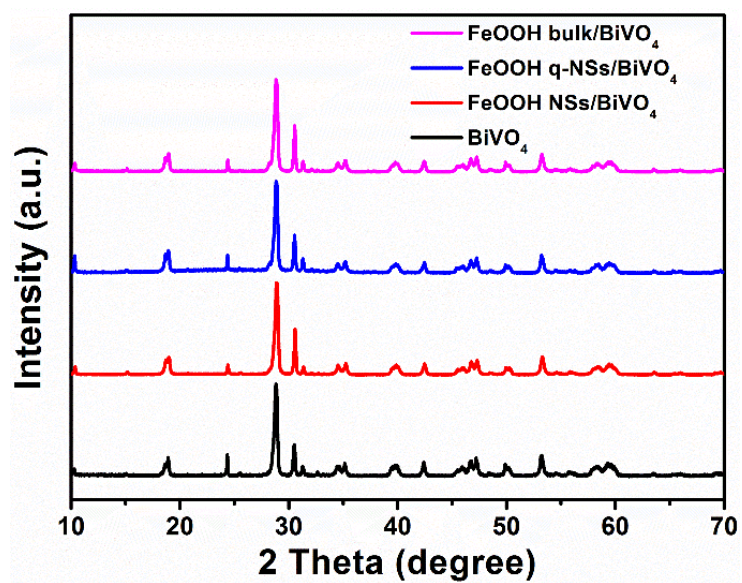


Fig. S7 XRD patterns of BiVO_4 and $\text{FeOOH}/\text{BiVO}_4$.

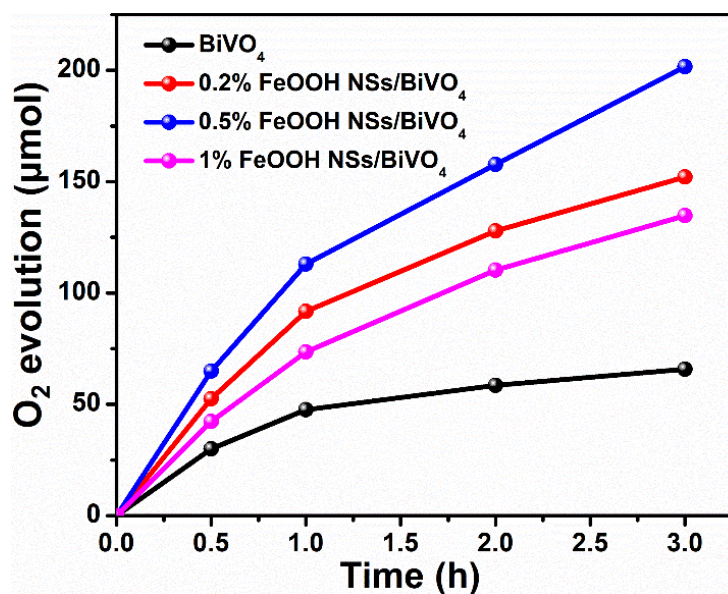


Fig. S8 Curves of visible-light O_2 evolution as a function of reaction time over BiVO_4 loaded with different amounts of FeOOH NSs .

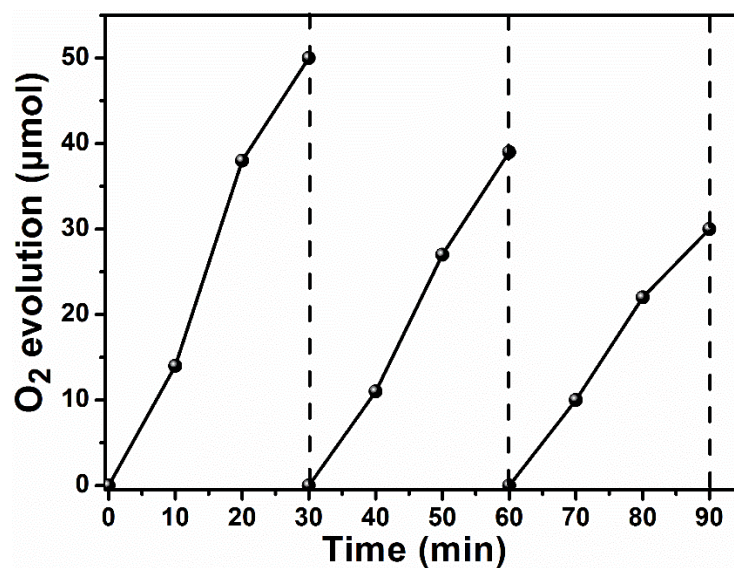


Fig. S9 Recycling stability of FeOOH NSs/BiVO₄ for photocatalytic oxygen evolution.

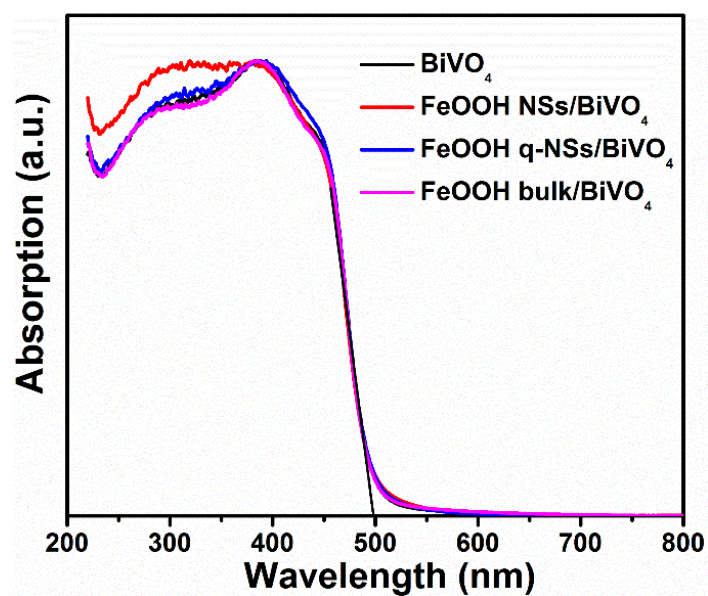


Fig. S10 UV-vis spectra of BiVO₄ and FeOOH/BiVO₄.

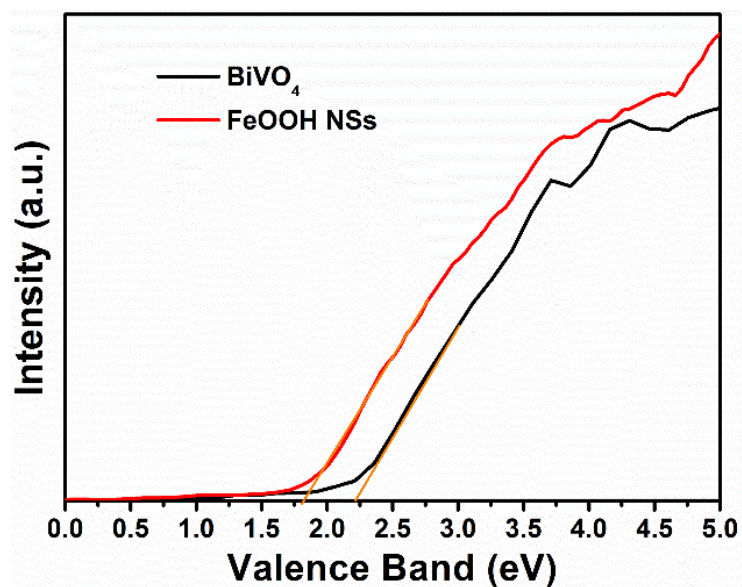


Fig. S11 Valence band spectra of BiVO_4 and FeOOH NSs.

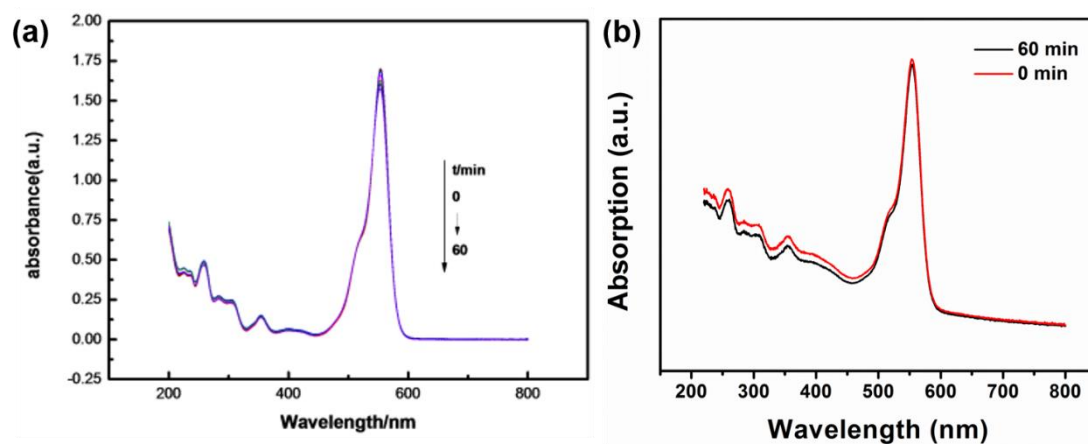


Fig. S12 (a) UV-vis spectra of RhB as a function of irradiation time without photocatalyst. (b) UV-vis spectra of RhB as a function of irradiation time in the presence of FeOOH NSs as a photocatalysts.

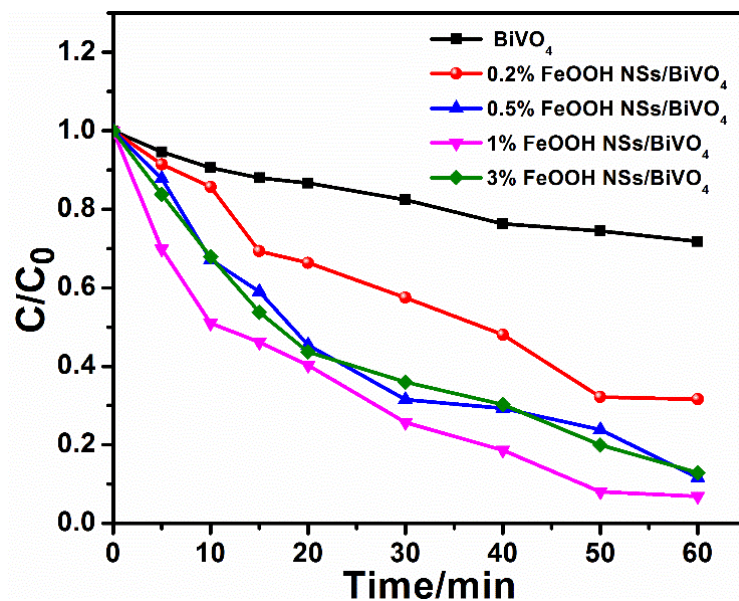


Fig. S13 Photodegradation of RhB over BiVO₄ with different loading amounts of FeOOH NSs.

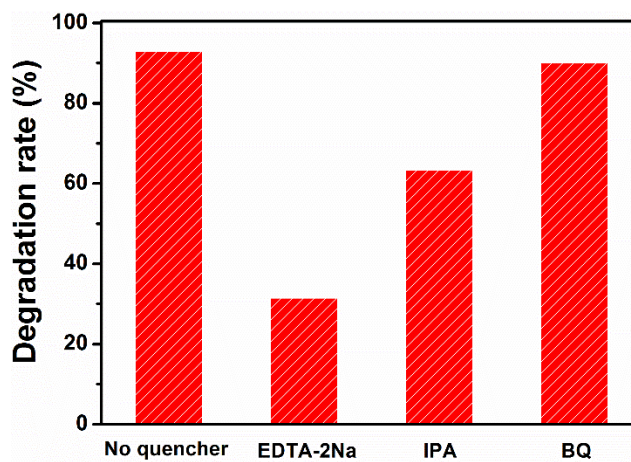


Fig. S14 Trapping experiment of active species during the photocatalytic degradation of RhB over FeOOH NSs/BiVO₄ under visible-light irradiation.

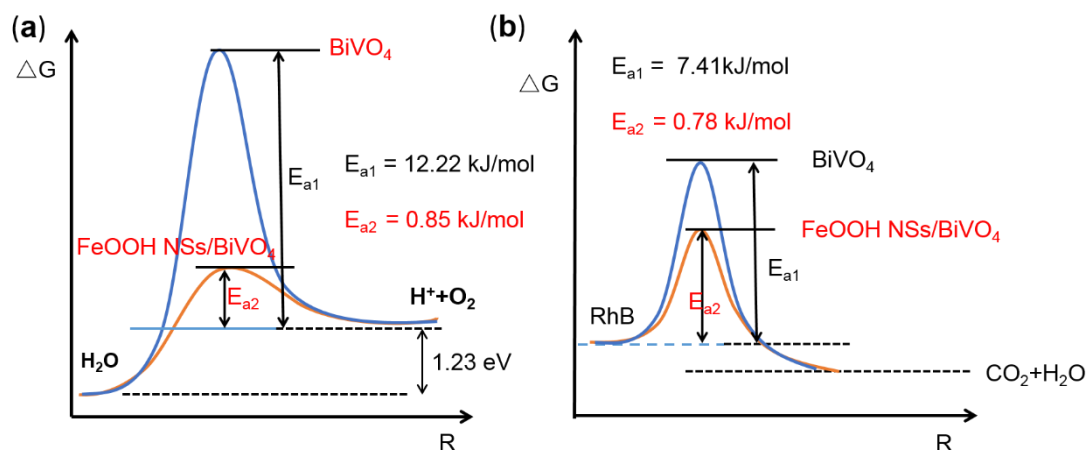


Fig. S15 (a) The apparent activation energy of O₂ evolution over BiVO₄ and FeOOH NSs/BiVO₄. (b) The apparent activation energy of the degradation of RhB over BiVO₄ and FeOOH NSs/BiVO₄.

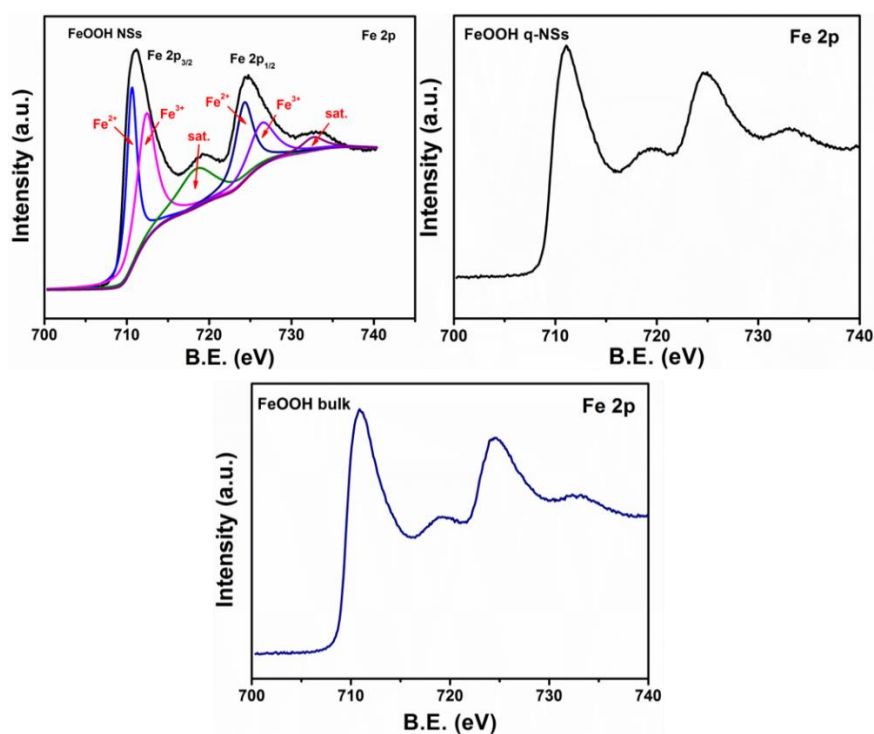


Fig. S16 XPS high resolution Fe 2p spectra of FeOOH NSs, FeOOH q-NSs and FeOOH bulk.

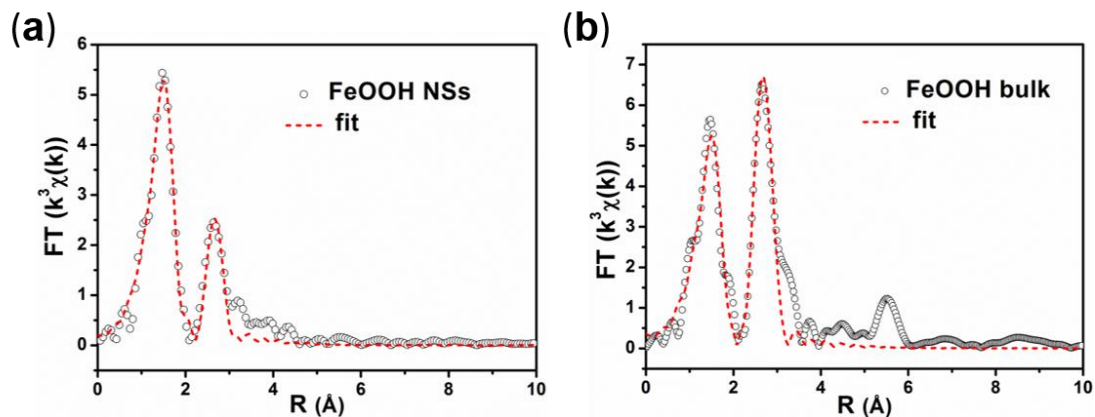


Fig. S17 EXAFS curves-fitting result of the a) FeOOH NSs and b) FeOOH bulk.

Table S1. EXAFS fitting results for the local structure parameters around Fe.

Sample	Path	N^a	R [Å] ^b	σ^2 [10 ⁻³ Å ⁻²] ^c	ΔE_0 [eV] ^d	R_f
β -FeOOH theory	Fe-O	6				
	Fe-Fe	4				
FeOOH bulk	Fe-O	5.9	1.98	11.0	-6.5	0.018
	Fe-Fe	3.9	3.05	7.2	2	
δ -FeOOH theory	Fe-O	6				
	Fe-Fe	2				
FeOOH NSs	Fe-O	5.4	1.97	10.8	-5.6	0.001
	Fe-Fe	1.6	3.04	8.6	-0.42	

^{a)} coordination number; ^{b)} distance; ^{c)} mean-square disorder; ^{d)} energy shift.

EXAFS fitting details: To obtain the quantitative structural parameters around Fe atoms in our samples, least-squares curve parameter fitting was performed using the ARTEMIS module of IFEFFIT software packages.¹ The amplitude reduction factor S_0 was treated as adjustable variable and the obtained value of 0.8 for Fe-foil was fixed in fitting the subsequent Fe edge data for the samples.

The fit was done on the k^3 -weighted EXAFS function $\chi(k)$ data from 3 to 12.3 Å⁻¹ in the R -range of 1.0–3.1 Å. The coordination numbers N , interatomic distances R , Debye-Waller factor σ^2 and the edge-energy shift ΔE_0 were allowed to run freely.

1 B. Ravel, M. Newville, *J. Synchrotron Radiat.* **2005**, *12*, 537.

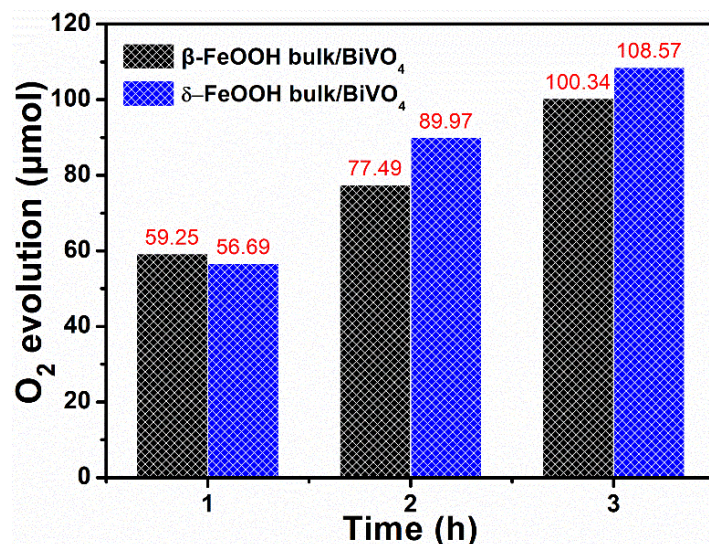


Fig. S18 Curves of visible-light O₂ evolution as a function of reaction time over β -FeOOH bulk/BiVO₄ and δ -FeOOH bulk/BiVO₄.

δ -FeOOH bulk was further synthesized in comparison with β -FeOOH bulk. Correspondingly, the δ -FeOOH bulk/BiVO₄ sample was also evaluated for photocatalytic O₂ evolutions under visible-light irradiation. Apparently, it was shown that photocatalytic oxygen activity of the two samples was almost the same, although the phases of the two bulk FeOOH were different.

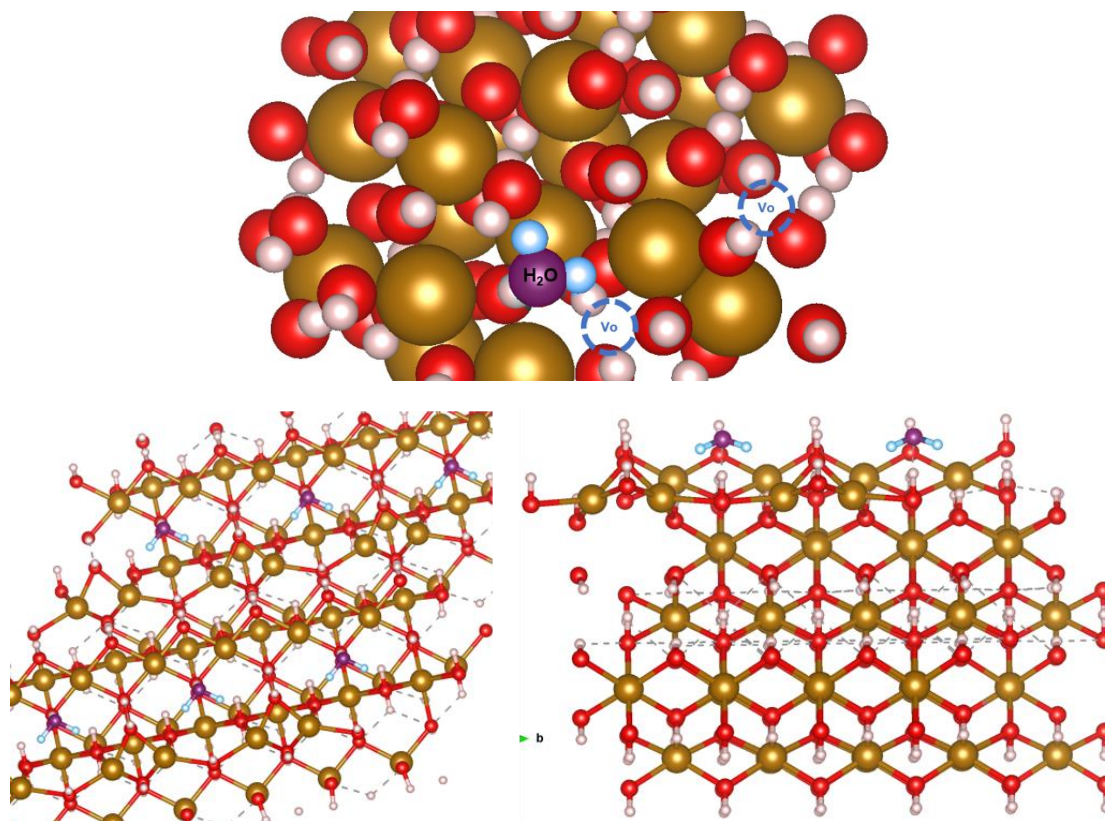


Fig. S19 Calculated surface atomic configurations for adsorbing water on H sites of ultrathin FeOOH with Vo.